Detection of acute kidney injury using hyperpolarized [1,4-$^{13}C_2$]fumarate

M. I. Kettunen[1], M. R. Clatworthy[2,3], T. H. Witney[1], D-E. Hu[1], B. W. Kennedy[1], S. E. Bohndiek[1], R. J. Mathews[2,3], F. A. Gallagher[1,4], K. G. Smith[2,3], and K. M. Brindle[1]

[1]Department of Biochemistry, University of Cambridge & Cancer Research UK Cambridge Research Institute, Cambridge, Cambridgeshire, United Kingdom, [2]Cambridge Institute for Medical Research, Cambridge, Cambridgeshire, United Kingdom, [3]Department of Medicine, University of Cambridge School of Clinical Medicine, Cambridge, Cambridgeshire, United Kingdom, [4]Department of Radiology, Addenbrooke's Hospital, University of Cambridge, Cambridge, Cambridgeshire, United Kingdom

Acute kidney injury (AKI), is a common and clinically important problem, affecting between 5 and 10% of all hospitalised patients, and 30 to 40% of those admitted to a critical care setting. Acute tubular necrosis (ATN), characterised histologically by flattening of tubular epithelium, tubular dilatation, and loss of tubular cell nuclei, and functionally by loss of electrolyte balance, leading to high urinary sodium, is the most common cause of AKI (1). The main important differential diagnoses in patients presenting with AKI is rapidly progressive glomerulonephritis (GN), which can occur secondary to autoimmune diseases. Treatment of the two conditions differs. Currently, however, there is no non-invasive test which differentiates ATN and GN, as the standard mode of imaging (ultrasound examination) demonstrates normal-sized, unobstructed kidneys in both cases.

Appearance of [1,4-$^{13}C_2$]malate signal following injection of hyperpolarized [1,4-$^{13}C_2$]fumarate has recently been suggested as a novel marker of necrosis (2-4). In this study, we have investigated whether hyperpolarized [1,4-$^{13}C_2$]fumarate could be a useful tool in the diagnosis of ATN, induced by folic acid administration (5), and whether this technique would allow ATN to be distinguished from acute inflammatory glomerulonephritis (GN).

Methods

Folic acid was dissolved in 150 mM sodium bicarbonate and administered intra-peritoneally at a dose of 250 mg/kg to C57BL/6 mice (n=26). Animals were imaged before folate injection and 10 h, 18 h, 26 h and 48 h post-injection (up to 3 time-point/animal). For GN, we used a model of lupus nephritis, the New Zealand Mixed (NZM)2410 lupus-prone congenic strain (n=6). For MR experiments, animals were anesthetized with intra-peritoneal injections of Hypnorm (VetaPharma)/Hypnovel(Roche)/dextrose-saline(4%:0.18%) in a 5:4:31 ratio (10 ml/kg body weight). [1,4-$^{13}C_2$]fumarate was polarized as described previously (2). All experiments were performed at 9.4 T using a 24-mm surface coil placed over the kidneys. ^{13}C spectroscopy and spectroscopic imaging were started 20 s after i.v. injection of 200 µl of fumarate. A single ^{13}C spectrum was first collected from the whole slice using a 600 µs sinc pulse with a nominal flip angle of 5° (TE 2 ms, spectral width 8000 Hz) and this was followed immediately by CSI (TR 20 ms, spectral width 8000 Hz, field of view 40x40 mm^2, data matrix 16x16). Blood samples were analyzed for serum urea levels after the MR experiments. H&E stained histological slides were used to assess the extent of kidney damage in a subset of animals at each time point. Tubulointerstitial damage was assessed by scoring three parameter; tubular necrosis, tubular dilatation, and cast formation. Scores were given as follows; involvement of 0 to 25% of tubules within each cortical or medullary high-powered field of view=1; 25 to 50%=2; 50 to 75%=3; 75 to 100%=4. All values are given as mean±SD.

Results

Only low levels of malate were detected in ATN animals before folate treatment; the malate/fumarate signal intensity ratio was 0.6 ± 0.9 %. In contrast, a prominent malate signal, that was localized to the kidneys was observed in animals treated with folate at 16-20 hours post-treatment, when the malate/folate ratio was 3.8 ± 1.7 % ($p<0.01$, Figs 1&2). At this time point weight loss, proteinuria and serum urea were elevated compared with baseline (Fig 3). There was also histological evidence of ATN, although this was not particularly severe. Interestingly, by 26 hours after folate acid treatment the malate/fumarate ratio decreased to 1.1 ± 0.7 % and remained at this level up to 48 hours post folic acid treatment. Both clinical and histopathological parameters describing the severity of ATN were greater at these later time points. No significant malate signals were observed in slices placed over the liver or heart at 18 h (n=3) suggesting that malate was produced in the kidneys. The malate/fumarate ratio was not significantly increased in NZM mice compared to control C57BL/6 animals. Consistent with this, these animals did not have significant histological features of ATN, although they did have proteinuria.

Discussion

Increased malate signals were observed 18 hours after folate treatment, at which time point there was histological evidence of tubular necrosis. A significant increase in the malate/fumarate ratio was not observed in mice with lupus nephritis. Thus, this technique could allow distinction of ATN from glomerular inflammation in the context of renal impairment. Interestingly, the malate/fumarate ratios had returned to near normal levels when the clinical and histological features of the disease were most severe. This suggests that when there is significant tubular necrosis, there may be loss of fumarase from damaged tubular cells which leads to loss of the malate signal at later time-points. Alternatively, the delivery of fumarate may be altered at the later time points.

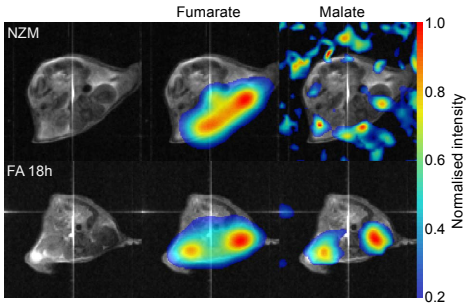

Figure 1. Images of the normalized signals from [1,4-$^{13}C_2$] fumarate and [1,4-$^{13}C_2$]malate following fumarate injection in NZM mouse and 18 h after folate treatment. Each image has been normalized separately to its maximum. Malate signal located to kidneys was observed following folate treatment.

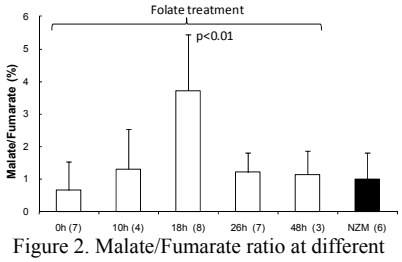

Figure 2. Malate/Fumarate ratio at different times following folate treatment and in NZM mice. Number of animals at each time point is given in parentheses.

Acknowledgements

This work was supported by a CRUK Programme Grant (to KMB). Hyperpolariser and research support were kindly provided by GE Healthcare.

References

1 Thadhani et al. NEJM 334:1448, 1996.
2. Gallagher et al. PNAS 106:19801, 2009.
3. Witney et al. BJC 103:1400, 2010.
4. Bohndiek et al. Mol. Cancer Ther, in press.
5. Zimmermann et al. Virchows Arch A Pathol Anat Histol 376:47, 1977.

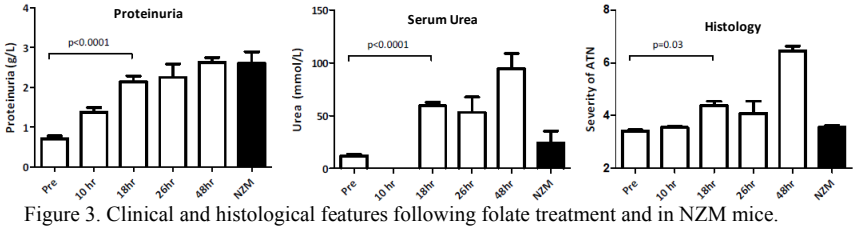

Figure 3. Clinical and histological features following folate treatment and in NZM mice.